PLEASE CITE THIS ARTICLE AS DOI: 10.1063/5.0146417

Theory of the Ion-Electron Temperature Relaxation Rate in Strongly Magnetized Plasmas

Louis Jose 1 and Scott D. Baalrud $^{2, \, a)}$

¹⁾ Applied Physics Program, University of Michigan, Ann Arbor, Michigan 48109, USA

OSDI Vivilear Engineering & Radiological Sciences, University of Michigan, Ann Arbor, Michigan 48109, USA

(Dated: 30 March 2023)

Recent works have shown that strongly magnetized plasmas characterized by having a gyrofrequency greater than the plasma frequency exhibit novel transport properties. One example is that the friction force on a test charge shifts, obtaining components perpendicular to its velocity in addition to the typical stopping power component antiparallel to its velocity. Here, we apply a recent generalization of the Boltzmann equation for strongly magnetized plasmas to calculate the ion-electron temperature relaxation rate. Strong magnetization is generally found to increase the temperature relaxation rate perpendicular to the magnetic field, and to cause the temperatures parallel and perpendicular to the magnetic field to not relax at equal rates. This, in turn, causes a temperature anisotropy to develop during the equilibration. Strong magnetization also breaks the symmetry of independence of the sign of the charges of the interacting particles on the collision rate, commonly known as the "Barkas effect". It is found that the combination of oppositely charged interaction and strong magnetization causes the ion-electron parallel temperature relaxation rate to be significantly suppressed, scaling inversely proportional to the magnetic field strength.

I. INTRODUCTION

Plasma generation typically results in a nonequilibrium state with electrons and ions at different temperatures, which subsequently equilibrate through energy exchange in Coulomb collisions. Understanding the rate of this relaxation is important to understanding plasma evolution. Here, we calculate the ion-electron temperature relaxation rate in strongly magnetized plasmas. Strongly magnetized plasmas are those in which the electron gyrofrequency exceeds the electron plasma frequency^{1,2}, i.e., $\beta = \omega_{ce}/\omega_{pe} > 1$, where $\omega_{ce} = eB/m_ec$ and $\omega_{pe} = \sqrt{4\pi e^2 n_e/m_e}$. Understanding electron-ion energy exchange at strong magnetization is interesting from the point of view of fundamental physics, as well as applications, including antimatter traps^{3,4}, magnetized ultracold neutral plasmas^{5–9}, non-neutral plasmas¹⁰, magnetized dusty plasmas¹¹, multi-MA accelerators¹², and magnetic confinement fusion 13.

In a weakly magnetized plasma, the ion temperature evolution owing to collisions with electrons can be obtained by taking the energy moment of the Boltzmann equation. For a spatially homogeneous plasma, this provides

$$\frac{dT_1}{dt} = -\nu \left(T_1 - T_2 \right) \tag{1}$$

where T_1 is the ion temperature, T_2 is the electron temperature and ν is the temperature relaxation rate. For a weakly magnetized plasma where the gyromotion of the particles occurs at a larger length scale than scattering,

the traditional Boltzmann collision operator ^{14} predicts the relaxation rate ${\rm as}^{15}$

$$\nu = \frac{32\sqrt{\pi}e^4n_2\ln\Lambda}{3m_1m_2(v_{T1}^2 + v_{T2}^2)^{3/2}}.$$
 (2)

Here, n_2 is the density of the electrons, m_1 and m_2 are the masses of the ions and electrons, respectively, $v_{T1} = \sqrt{2T_1/m_1}$ and $v_{T2} = \sqrt{2T_2/m_2}$ are the thermal velocities, and $\ln \Lambda$ is the Coulomb logarithm.

This work focuses on the opposite limit, where gyromotion occurs at a smaller length scale than scattering. In this case, the relaxation rate was obtained using the recently developed generalized Boltzmann kinetic theory for strongly magnetized plasmas¹⁶. The Boltzmann equation is generalized in this theory to account for the Lorentz force acting on particles during binary collisions. The theory was previously validated by comparing the friction force on a test charge moving through strongly magnetized plasmas with data from first-principles molecular dynamics (MD) simulations¹⁷ Strong magnetization was found to give rise to novel physics, such as the friction force not being antiparallel to the velocity and having additional perpendicular components 16,18-23. This was found to give rise to nonintuitive features, such as an increase in the gyroradius of a test charge slowing down in strongly magnetized plasma^{17,21}. Strong magnetization was also discovered to cause a Barkas effect where the collision rate depends on the sign of charges of interacting particles²⁴. As a result, it was found that the electrical resistivity and conductivity of the electron-ion plasma differed significantly from the positron-ion plasma, which is not a property of weakly magnetized plasmas.

In this work, the ion-electron temperature relaxation rate is calculated from the energy exchange density of

a) Electronic mail: baalrud@umich.edu

PLEASE CITE THIS ARTICLE AS DOI: 10.1063/5.0146417

a test ion interacting with background electrons. It is found that when the plasma is strongly magnetized. the parallel and perpendicular relaxation rates are no longer equal, causing a temperature anisotropy to form. Cases are considered for both attractive (electron-ion) and repulsive (positron-ion) interactions. The calculation predicts that the relaxation rates are qualitatively and quantitatively different in each case. The difference between the parallel and perpendicular relaxation rates for attractive collisions is much more significant than for repulsive collisions. For repulsive interactions, strong magnetization increases both the parallel and perpendicular relaxation rates and becomes constant at extreme values. In contrast, for attractive interactions, the parallel relaxation rate is inversely proportional to the magnetization strength (β) in the strongly magnetized regime. The relaxation rates are also dependent on the Coulomb coupling strength, $\Gamma = (e^2/a)/(k_BT)$, where $a = [3/(4\pi n)]^{1/3}$ is the Wigner-Seitz radius in addition to the magnetization strength, β . Three values of Γ are considered: 0.1, 1 and 10.

Understanding the thermal relaxation of ions in strongly magnetized plasmas has many applications, including the antimatter experiments at Antihydrogen Laser Physics Apparatus (ALPHA), which synthesizes antihydrogen from antiprotons and positrons^{25,26} After slowing and trapping, the collisional temperature relaxation of antiprotons occurs in two stages. First, antiprotons are collisionally cooled with electrons. Second, antiprotons are brought into thermal equilibrium with positrons during the recombination pro $cess^{25-27}$. For typical experimental conditions, electrons and positrons are strongly magnetized and have magnetization strengths around few hundred ($\beta \sim 300$). Since both ion-electron and ion-positron interactions are important, the results for attractive (+-) and repulsive (++) potentials are both relevant to this experiment.

Previous works calculating the temperature relaxation in strongly magnetized plasmas employed methods such as Fokker-Plank equations²⁸, linear-response theory²⁹, force correlation methods^{30,31}, binary collisions^{32–34}, and other perturbation methods³⁵. These works showed that the magnetic field enhances the relaxation rate, which is proportional to the logarithm of the magnetic field strength. However, all these methods were limited to weakly coupled plasmas ($\Gamma \ll 1$) and to the transport regimes where the gyroradius is smaller than the Debye length but larger than the distance of the closest approach.

This work extends the calculation of temperature relaxation to extreme magnetization regimes where the gyroradius is smaller than the distance of the closest approach. Instead of relying on perturbative methods or weak interaction approximations to calculate the energy change during the binary collision events, the particle trajectories are numerically evaluated with high numerical precision. This work also extends the calculation of temperature relaxation to the strongly coupled

regime using an effective potential theory called the potential of mean force 36,37 . This makes the result applicable to non-neutral plasmas, 10 antimatter trap plasmas, 3,4 and mangetized ultracold neutral plasmas $^{5-9}$ which have strongly coupled components.

The outline of this paper is as follows. In Sec. II, the theoretical formulation of energy exchange between a test charge and strongly magnetized background plasma is described. Section III discusses the influence of coupling strength, angle between the test charge velocity and magnetic field (i.e., its orientation θ), and the sign of the test charge on the energy exchange density. In Sec. IV, the ion-electron temperature relaxation rate is obtained from the energy exchange density of the test charge. Section V discusses the parallel and perpendicular temperature evolution of warm ions collisionally relaxing on a heat bath of strongly magnetized electrons.

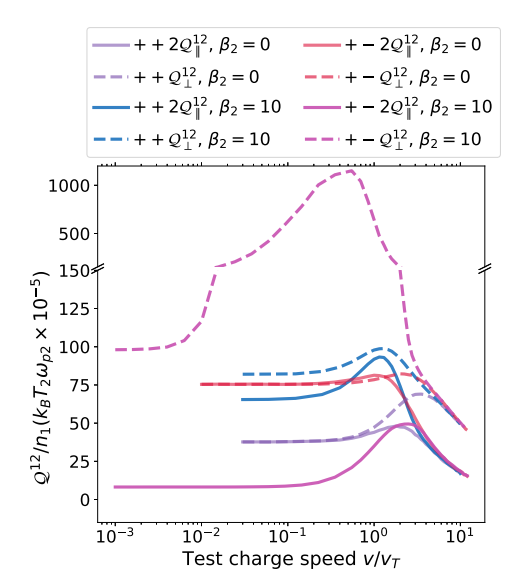


FIG. 1: Energy exchange density components (\mathcal{Q}_{\perp}^{12} and $\mathcal{Q}_{\parallel}^{12}$) of the like charged (++) and opposite charged (+-) cases for coupling strength, $\Gamma_2=1$ and orientation $\theta=22.5^{\circ}$. Note that the break in the vertical axis signifies a switch from linear to logarithmic scale.

II. THEORY

The temperature relaxation rate of a distribution of ions is closely related to the energy exchange density of a test ion slowing down on electrons ^{38,39}. This is because the heavy mass of the ions makes the ion velocity dis-

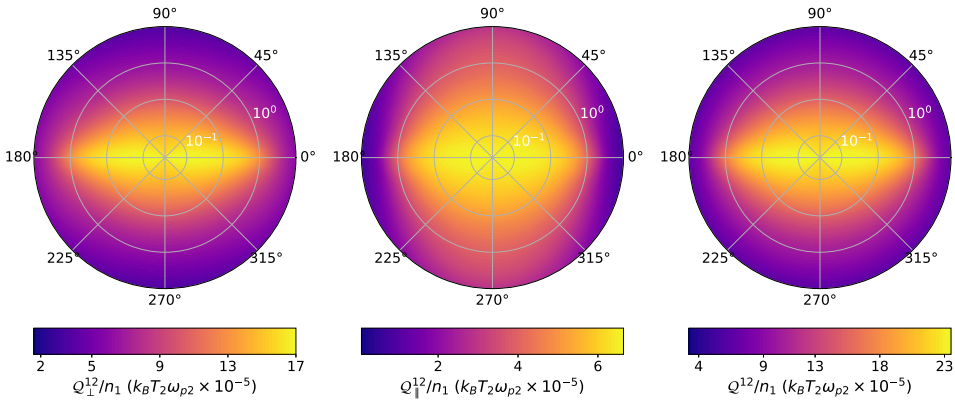


FIG. 2: Polar plots of the energy exchange density components $(Q_{\perp}^{12}, Q_{\parallel}^{12} \text{ and } Q^{12})$ of the like-charged (++) interaction at $\Gamma_2 = 0.1$ and $\beta_2 = 10$. The radial axis is the speed of the test charge (v_1/v_{T_2}) and the angle is the phase angle that the test charge velocity makes with the direction of the magnetic field (θ) .

tribution very narrow compared to the electron velocity distribution. In this limit, the ion velocity distribution can be modeled as a Dirac delta function, which is mathematically equivalent to a single particle. We first calculate the energy exchange density of a single test charge and later use it to calculate the temperature relaxation rate.

The energy exchange of a test charge that moves with a velocity, \mathbf{v}_0 in a sea of background electrons can be obtained by taking the energy moment of the collision operator $(Q^{12} = \int d^3\mathbf{v}_1m_1(\mathbf{v}_1 - \mathbf{v}_0)^2C/2)$. The velocity distribution of a single test charge can be modeled as a Maxwellian distribution with flow (\mathbf{v}_0) , and zero temperature. This limit is the Dirac delta function $(f_1 = n_1\delta^3(\mathbf{v}_1 - \mathbf{v}_0))$. Thus for a single test charge, the energy exchange moment is Q^{12}/n_1 . Here, species 1 is ions and species 2 is the background electron or positron distribution. Using the generalized collision operator $(GCO)^{16}$, the energy exchange density is

$$\frac{\mathcal{Q}^{12}}{n_1} = \frac{n_2 m_1}{2\pi^{3/2} v_{T2}^3} \int d^3 \mathbf{v}_2 ds |\mathbf{u} \cdot \hat{\mathbf{s}}| (\mathbf{v}_0' - \mathbf{v}_0)^2 e^{-v_2^2/v_{T2}^2}.$$
(3)

Here, the surface integral is on the surface of the collision volume, and the background plasma is assumed to be a Maxwellian distribution with thermal velocity $v_{T2} = \sqrt{2k_BT_2/m_2}$. The post collision velocity of the test charge (\mathbf{v}_0') is the input to the collision operator and is obtained by solving equations of motion of the colliding particles inside the collision volume.

The ratio of the mass of the test charge (m_1) to the mass of the background particles (m_2) is set at 1000; $m_r=m_1/m_2=1000$. As the test charge is much more massive, the Lorentz force has little impact on its motion.

As a result, the equations of motion can be simplified as 16

$$(m_1 + m_2) \frac{d\mathbf{V}}{dt} = e\left(\frac{\mathbf{V}}{c} \times \mathbf{B}\right) - \frac{e \, m_{12}}{m_2} \left(\frac{\mathbf{u}}{c} \times \mathbf{B}\right), (4a)$$

$$m_{12} \frac{d\mathbf{u}}{dt} = -[\pm \nabla \phi(r)] + \frac{e \, m_{12}^2}{m_2^2} \left(\frac{\mathbf{u}}{c} \times \mathbf{B}\right)$$

$$-\frac{e \, m_{12}}{m_2} \left(\frac{\mathbf{V}}{c} \times \mathbf{B}\right). \tag{4b}$$

where $\mathbf{V} = (m_1\mathbf{v}_0 + m_2\mathbf{v}_2)/(m_1 + m_2)$ is the center of mass velocity, $m_{12} = m_1m_2/(m_1 + m_2)$ is the reduced mass, and $\mathbf{u} = \mathbf{v}_0 - \mathbf{v}_2$ is the relative velocity. Here, $\phi(r)$ is the potential of mean force 36,37,40 . For a weakly coupled plasma, the potential of mean force is the Debye-Hückel potential. The potential of mean force was obtained using the hypernetted-chain approximation for one component plasma 41 . The plus (+) sign of the potential is for the like-charged case and the minus (-) is for the opposite-charged case. The traditional Boltzmann theory does not include a magnetic field in the equations of motion and uses a bare Coulomb potential as the interaction potential. This simplifies the equations of motion and leads to the analytical form of temperature relaxation rate described in Eq. (2).

The energy exchange density can be split into components parallel and perpendicular to the magnetic field $(\mathcal{Q}_{\parallel}^{12} = \int d^3\mathbf{v}_1 m_1(\mathbf{v}_{1\parallel} - \mathbf{v}_{0\parallel})^2 \mathcal{C}/2)$ and $(\mathcal{Q}_{\perp}^{12} = \int d^3\mathbf{v}_1 m_1(\mathbf{v}_{1\perp} - \mathbf{v}_{0\perp})^2 \mathcal{C}/2)$. The two components add to give the total energy exchange density, i.e., $\mathcal{Q}^{12} = \mathcal{Q}_{\parallel}^{12} + \mathcal{Q}_{\perp}^{12}$. In a weakly magnetized plasma, $\mathcal{Q}_{\parallel}^{12} = \frac{1}{2}\mathcal{Q}_{\perp}^{12}$ in the limit of a low test charge speed. Separating the parallel and perpendicular components will enable an analysis of temperature anisotropy formation in strongly magnetized plasmas.

Physics of Plasmas

This is the author's peer reviewed, accepted manuscript. However, the online version of record will be different from this version once it has been copyedited and typeset PLEASE CITE THIS ARTICLE AS DOI: 10.1063/5.0146417

Similar to the case of the friction force calculation 16,17,24 , the energy moment integral is solved using the adaptive Monte Carlo integration code VEGAS 42,43 and the equations of motion of the colliding particles were solved using the "DOP 853" method 44 . The tolerance for the trajectory calculations was set to 10^{-8} . The collision volume was taken as a sphere. The radius of the spherical collision volume for coupling strengths $\Gamma_2=0.1,1,$ and 10 was taken to be 6.39a and 2.88a,2.74a respectively. These radii were chosen to ensure minimal interaction at the surface of the collision volume.

III. RESULTS

Figure 1 shows example profiles of the energy exchange density, in this case for a background coupling strength of $\Gamma_2=1$ and an angle of $\theta=22.5^\circ$ between the test particle velocity and magnetic field. The energy exchange density in the parallel and perpendicular directions gives the thermalization rate of a cool beam of ions in those directions. Its value in the perpendicular direction is expected to be double that of the parallel direction because there are two degrees of freedom compared to one. When the parallel and perpendicular energy exchange densities do not satisfy this criterion, it leads to different relaxation rates in each direction, which can generate a temperature anisotropy.

For low speeds, the energy exchange densities are independent of the speed of the test charge (see Fig. 1). In the unmagnetized cases, the low-speed value of the perpendicular energy exchange density is double that of the parallel. This is the usual expectation of weakly magnetized plasma, where the electrons and ions relax isotropically in the limit there is no relative drift. However, in the case of strongly magnetized plasma, the limiting values of the perpendicular energy exchange density are greater than double that of the parallel. Thus, strong magnetization is expected to lead to the development of temperature anisotropy during the relaxation. This difference in the perpendicular and parallel energy exchange densities is significantly enhanced for attractive collisions compared to repulsive. In fact, for $\beta_2 = 10$, Q_{\perp} is more than an order of magnitude greater than $2Q_{\parallel}$, suggesting that electron-ion energy exchange is much faster in the perpendicular direction.

The difference between attractive and repulsive collision rates is a significant, and perhaps surprising, effect that is often called the "Barkas" effect. Collisions in standard plasma kinetic theories are based on either the Rutherford scattering cross section in Boltzmann-type models, or on the linear dielectric response function in Lennard-Balescu type models. Both cases predict that the collision rate has no dependence on the sign of the interacting charges, since only the square of the charges enters the theory. It has previously been shown that a Barkas effect arises in strongly coupled plasmas. ⁴⁵ The explanation for this is that screening associated with the

potential of mean force leads to a difference in the scattering cross section when the relative speeds of particles are small, corresponding to the close-interaction regime. Here, we observe a Barkas effect in a moderately coupled plasma ($\Gamma_2 = 1$), but which also depends strongly on the degree of magnetization. It is expected that, like the strong coupling case, the origin of the effect is a dependence on the sign of interacting charges in close collisions. Attractive collisions are generally observed to lead to closer interactions that occur over a much longer timescale, including occurrences of pseudo-bound states, than repulsive collisions. It is noteworthy that previous work studying the influence of strong magnetization from a linear response perspective does not predict a Barkas effect. 21,22 The reason is similar to unmagnetized plasmas: the linear dielectric response does not consider close interactions, and therefore is independent of the sign of the charges. This emphasizes the need for a particlebased collision model at sufficiently strong magnetization strength.

The Barkas effect is more significant in the case of small-speed large-angle scattering than for high-speed small-angle scattering. Thus, the energy exchange density enhancement due to the Barkas effect is absent at high speeds of the test charge, as indicated by the merging of the like-charged and oppositely-charged curves at high speed; see Fig. 1. Similarly, the curves for the strongly magnetized conditions merge with those for unmagnetized conditions at high speeds. This is because the collisions of a high-speed test charge happen at a faster time scale than the gyromotion of the electrons, nullifying the strong magnetization effect.

Figures 2, 3 and 4 show results of computations of the energy exchange density components for different orientations of the test charge velocity with respect to the direction of the magnetic field (θ) . Figures 2 and 3 show results for like-charged interactions at coupling strengths $\Gamma_2=0.1$ and $\Gamma_2=1$ and Fig. 4 for oppositely-charged interactions at coupling strength $\Gamma_2=1$. The energy exchange density not only depends on the speed and sign of the ion charge, but also on θ . However, at very low speeds Q_\parallel^{12} and Q_\perp^{12} are observed to become independent of θ .

Figure 2 shows that at weak coupling $(\Gamma_2=0.1)~Q_\parallel^{12}$ is largely independent of θ at any speed, while Q_\parallel^{12} is peaked along the magnetic field $(\theta=0,180^\circ).$ Here, both Q_\parallel^{12} and Q_\perp^{12} take maximal values in the low speed limit, having long flat plateaus at low speed. In contrast, Fig. 3 shows that at moderate coupling $(\Gamma_2=1)$, both Q_\parallel^{12} and Q_\perp^{12} depend strongly on θ , with the peak value of each being along the magnetic field $(\theta=0,180^\circ)$ at a speed of a few thermal speeds.

The comparison of Figs. 3 and 4 show that for attractive interactions (+-), the peak value of Q_{\perp}^{12} is significantly larger than all other cases and occurs at a speed slightly less than the thermal speed. This suggests that the energy exchange in the perpendicular direction is very



PLEASE CITE THIS ARTICLE AS DOI: 10.1063/5.0146417

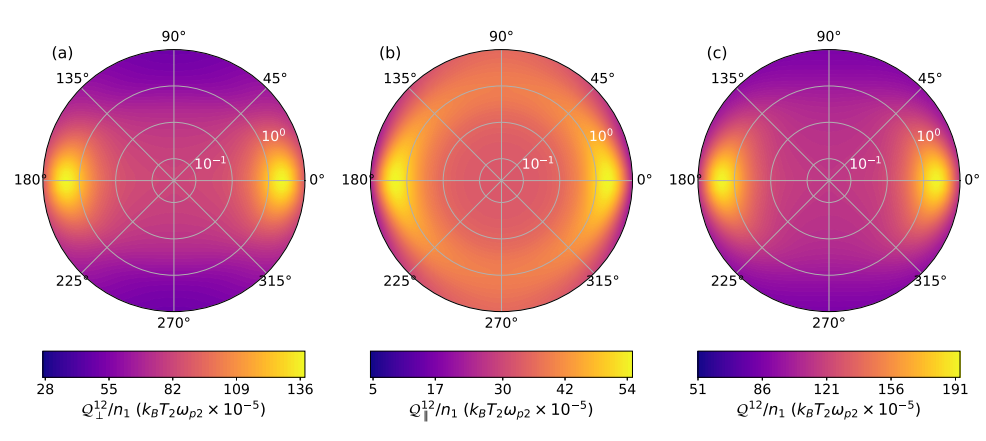


FIG. 3: Polar plots of the energy exchange density components $(\mathcal{Q}_{\perp}^{12}, \mathcal{Q}_{\parallel}^{12} \text{ and } \mathcal{Q}^{12})$ of the like-charged (++) interaction at $\Gamma_2 = 1$ and $\beta_2 = 10$. The radial axis is the speed of the test charge (v_1/v_{T_2}) and the angle is the phase angle that the test charge velocity makes with the direction of the magnetic field (θ) .

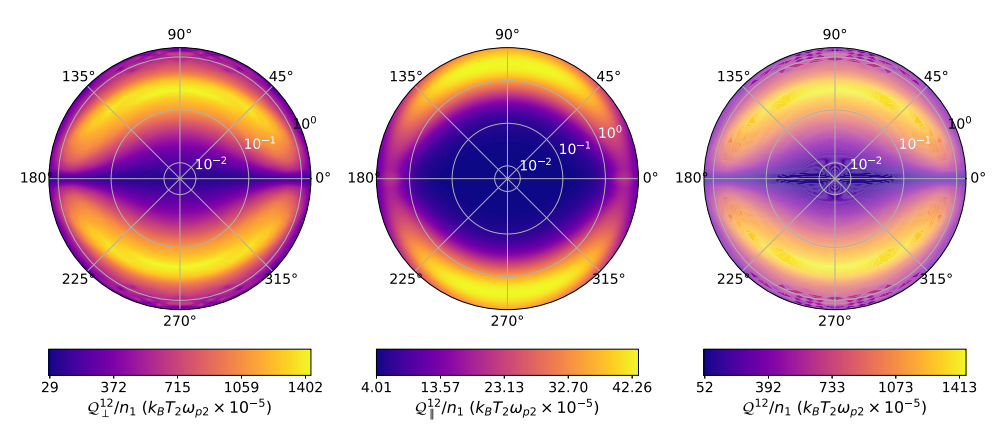


FIG. 4: Polar plots of the energy exchange density components $(\mathcal{Q}_{\perp}^{12}, \mathcal{Q}_{\parallel}^{12})$ and \mathcal{Q}^{12} of the opposite-charged (+-) interaction at $\Gamma_2 = 1$ and $\beta_2 = 10$. The radial axis is the speed of the test charge (v_1/v_{T_2}) and the angle is the phase angle that the test charge velocity makes with the direction of the magnetic field (θ) .

rapid for an oppositely charged beam especially when moving slightly slower than the thermal speed of the electrons. In this case, the peak value of all energy exchange density components is when the test charge moves perpendicular to the magnetic field. This contrasts with the repulsive (++) case, where the peak values occur when the test charge moves along the magnetic field. This observation is similar to the friction force, where the oppositely charged test charge (+-) experiences maximum friction when moving perpendicular to the magnetic field, while the like-charged case is peaked when moving par-

allel to the magnetic field. 24 The increase of the peak value from the plateau value in the low speed limit is also significant in the +- case.

IV. TEMPERATURE RELAXATION

The energy exchange density for a test charge was discussed in the previous section. Here, we extend the calculation to a distribution of ions with a finite temperature and apply the result to model the evolution of

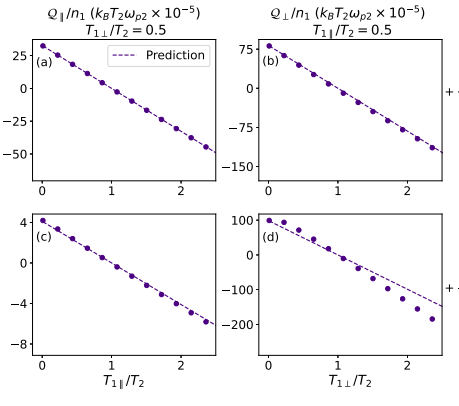


FIG. 5: Energy exchange density of an ion distribution as a function of its parallel [(a) and (c) for fixed $T_{\perp}/T_2 = 0.5$] and perpendicular [(b) and (d) for fixed $T_{\parallel}/T_2 = 0.5$ temperatures. Circles denote solutions of Eqs. (10) and (11). The dashed line shows the linear prediction from Eqs. (14) and (15). The top row is for the case of like-charged collisions and bottom row is for the case of opposite-charged collisions. Here, the coupling strength is $\Gamma_2 = 1$ and magnetization is $\beta_2 = 10.$

the ion distribution as it relaxes with a strongly magnetized electron distribution held at a fixed temperature (i.e., a heat bath). Since strong magnetization causes an anisotropy in the energy exchange density, we consider an anisotropic Maxwellian distribution for ions

$$f_1 = \frac{n_1}{\pi^{3/2} v_{T_{1}}^2 v_{T_{1}}} e^{-v_{1\parallel}^2 / v_{T_{1}\parallel}^2} e^{-v_{1\perp}^2 / v_{T_{1\perp}}^2}.$$
 (5)

Here, $v_{T_1\parallel}=\sqrt{2k_BT_1\parallel/m_1}$ and $v_{T_1\perp}=\sqrt{2k_BT_1\perp/m_1}$ are parallel and perpendicular ion thermal speeds. Here, we note that the anisotropic Maxwellian is an assumed form for the distribution function that is expected to be accurate particularly when the difference between the electron and ion temperatures is relatively small. Assuming this form, the parallel energy exchange density

$$Q_{\parallel} = \frac{1}{2} m_1 \int d^3 \mathbf{v}_1 d^3 \mathbf{v}_2 ds |\mathbf{u} \cdot \hat{\mathbf{s}}| (v_{1\parallel}^{\prime 2} - v_{1\parallel}^2) f_1 f_2$$
 (6)

Using, $v_{1\parallel}'^2 - v_{1\parallel}^2 = (v_{1\parallel}' - v_{1\parallel})^2 + 2v_{1\parallel}(v_{1\parallel}' - v_{1\parallel})$, this can equivalently be expressed as

$$Q_{\parallel} = \frac{1}{2} m_1 \int d^3 \mathbf{v}_1 d^3 \mathbf{v}_2 ds |\mathbf{u} \cdot \hat{\mathbf{s}}| \left[(v'_{1\parallel} - v_{1\parallel})^2 + 2v_{1\parallel} (v'_{1\parallel} - v_{1\parallel}) \right] f_1 f_2.$$
 (7)

On rewriting $f_1 = \int \delta^3(\mathbf{v}_1 - \mathbf{v}_0) f_1(\mathbf{v}_0)$, and evaluating the $d^3\mathbf{v}_1$ integral

$$\begin{aligned} \mathcal{Q}_{\parallel} &= \int d^3 \mathbf{v}_0 f_1(\mathbf{v}_0) \int d^3 \mathbf{v}_2 ds |\mathbf{u} \cdot \hat{\mathbf{s}}| \frac{1}{2} m_1 (v_{0\parallel}' - v_{0\parallel})^2 f_2 \\ &+ \int d^3 \mathbf{v}_0 f_1(\mathbf{v}_0) \int d^3 \mathbf{v}_2 ds |\mathbf{u} \cdot \hat{\mathbf{s}}| m_1 v_{0\parallel} (v_{0\parallel}' - v_{0\parallel}) f_2 \& \end{aligned}$$

Assuming an isotropic Maxwellian distribution of electrons, $f_2 = n_2/(\pi^{3/2}v_{T_2}^3) \exp(-v_2^2/v_{T_2}^2)$ and using the definitions of energy exchange density, Eq. (3), and friction force of the test charge charge 24

$$\mathbf{F} = \frac{n_2 m_1}{\pi^{3/2} v_T^3} \int d^3 \mathbf{v}_2 \int_{S_-} ds \, |\mathbf{u} \cdot \hat{\mathbf{s}}| (\mathbf{v}_0' - \mathbf{v}_0) e^{-v_2^2 / v_T^2}, \quad (9)$$

this can be further simplified to

$$Q_{\parallel} = \int d^3 \mathbf{v}_0 f_1(\mathbf{v}_0) Q_{\parallel}^{12} / n_1 + \int d^3 \mathbf{v}_0 f_1(\mathbf{v}_0) F_{\parallel} v_{0\parallel}(10)$$

Similarly, the perpendicular energy exchange density is

$$Q_{\perp} = \int d^3 \mathbf{v}_0 f_1(\mathbf{v}_0) Q_{\perp}^{12} / n_1 + \int d^3 \mathbf{v}_0 f_1(\mathbf{v}_0) \mathbf{F}_{\perp} \cdot \mathbf{v}_0 (11)$$

Finally, the parallel and perpendicular energy moments of the Boltzmann equation connect the energy exchange densities to the rate of change of the respective temper-

$$n_1 k_B \frac{dT_{1\perp}}{dt} = Q_{\perp},$$
 (12)

$$n_1 k_B \frac{dT_{1\perp}}{dt} = \mathcal{Q}_{\perp}, \qquad (12)$$

$$\frac{1}{2} n_1 k_B \frac{dT_{1\parallel}}{dt} = \mathcal{Q}_{\parallel}. \qquad (13)$$

Considering the common situation that the electron and ion temperatures are not dramatically different (i.e., $T_1/T_2 \sim 1$), an analytic approximation of the temperature evolution can be obtained by assuming a linear dependence of the form: $Q_{\parallel} \propto (1-T_{1\parallel}/T_2)$ and $Q_{\perp} \propto (1 - T_{1\perp}/T_2)$. In the limit that the parallel or perpendicular temperature is zero, the energy exchange density should asymptote to the value for that of a test charge in the limit of zero speed, i.e., $Q_{\perp}(T_{1\perp} \rightarrow 0) =$ $Q_{\perp}^{12}(v_1 \to 0)$ and $Q_{\parallel}(T_{1\parallel} \to 0) = Q_{\parallel}^{12}(v_1 \to 0)$. In the limit that the ion parallel or perpendicular temperature is equal to that of the electron temperature, the energy exchange in the respective directions goes to zero, i.e., $Q_{\perp}(T_{1\perp} \to T_2) = 0$ and $Q_{\parallel}(T_{1\parallel} \to T_2) = 0$. With these two limiting cases and the assumption of a linear dependence on the temperature ratio, the parallel and perpendicular energy exchange densities for a distribution of ions can be related to the test particle values in the low speed limit

$$Q_{\parallel} = \lim_{v_1 \to 0} Q_{\parallel}^{12}(v_1) \left(1 - \frac{T_{1\parallel}}{T_2} \right)$$
 (14)

$$Q_{\perp} = \lim_{v_1 \to 0} Q_{\perp}^{12}(v_1) \left(1 - \frac{T_{1\perp}}{T_2} \right) \tag{15}$$

where $\mathcal{Q}_{\parallel}^{12}(v_1)$ and $\mathcal{Q}_{\parallel}^{12}(v_1)$ are the components of the test particle energy exchange density.

PLEASE CITE THIS ARTICLE AS DOI: 10.1063/5.0146417

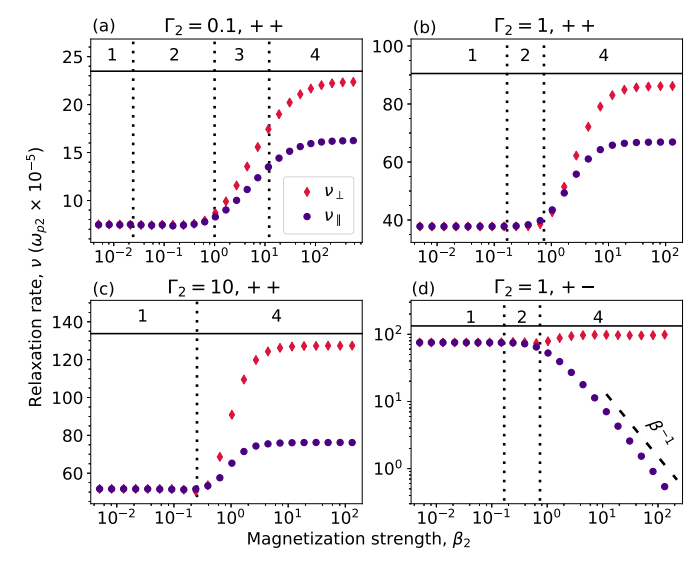


FIG. 6: The ion-electron temperature relaxation rates for like-charged collisions [(a) $\Gamma_2 = 0.1$, (b) $\Gamma_2 = 1$ and (c) $\Gamma_2 = 10$] and opposite charged collisions [(d) $\Gamma_2 = 1$]. The red circles are the perpendicular relaxation rates and the blue circles are the parallel relaxation rates. Vertical dotted lines delineate transitions between the four transport

This linear model is overall in good agreement with direct numerical integration of Eqs. (10) and (11) for ionelectron temperature ratios near 1; as shown in Fig. 5. The small deviation of Q_{\perp} from the linear prediction in the attractive interaction case (+-) might be because the \mathcal{Q}_{\perp}^{12} curve does not plateau to a constant value until very small speeds are reached $(v/v_T \lesssim 10^{-2})$; see Fig. 1. The energy exchange density of the ions having a linear dependence on the ion temperature is equivalent to saying that the temperature relaxation rate is independent of the ion temperature. From Eqs. (12)–(15), we get

$$\frac{dT_{1\perp}}{dt} = -\nu_{\perp} (T_{1\perp} - T_2) \qquad (16)$$

$$\frac{dT_{1\perp}}{dt} = -\nu_{\perp} \left(T_{1\perp} - T_2 \right)$$

$$\frac{dT_{1\parallel}}{dt} = -\nu_{\parallel} \left(T_{1\parallel} - T_2 \right)$$

$$(16)$$

where,

$$\nu_{\perp} = \lim_{v_1 \to 0} \frac{\mathcal{Q}_{\perp}^{12}(v_1)}{n_1 k_B T_2},\tag{18}$$

$$\nu_{\perp} = \lim_{v_1 \to 0} \frac{\mathcal{Q}_{\perp}^{12}(v_1)}{n_1 k_B T_2}, \qquad (18)$$

$$\nu_{\parallel} = 2 \lim_{v_1 \to 0} \frac{\mathcal{Q}_{\parallel}^{12}(v_1)}{n_1 k_B T_2}. \qquad (19)$$

The temperature relaxation rates ν (linear order) depend only on the low speed value of Q^{12} . Since the low speed value of Q^{12} does not depend on the orientation of the test charge with respect to the magnetic field, the calculation of the temperature relaxation can be extended to higher β values very efficiently. Instead of creating the whole polar plot and integrating, Q^{12} was calculated for a fixed orientation $\theta = 22.5^{\circ}$, at very low speed $(\approx 10^{-2}v_{T2})$ for different magnetization strengths. The results of this calculation for different coupling strengths are shown in Fig. 6

The figure also indicates regimes that have previously been predicted to delineate when changes in transport properties occur.2 These are defined by comparing the electron gyroradius $(r_c = \sqrt{k_B T_2/m_2}/\omega_{c2})$ with other fundamental length scales including the Coulomb collision mean free path (λ_{col}) , Debye length $(\lambda_D =$ $\sqrt{k_B T_2/4\pi e^2 n_2}$), and Landau length $(r_L = \sqrt{2}e^2/k_B T_2)$. The four regimes are: 1) The unmagnetized regime $(r_c >$ $\lambda_{\rm col}$): Here, the gyroradius is larger than the Coulomb collision mean free path. Thus, the magnetic field is not expected to influence transport. 2) The weakly magnetized regime (max(λ_D, a) < $r_c < \lambda_{\rm col}$): Here, the magnetic field influences transport by acting on the distribution function. However, collisions between particles occur at microscopic scales (less than the Debye length) are not influenced by gyromotion, so the collision operator does not explicitly depend on the magnetic field. 3) The strongly magnetized regime $(r_L < r_c < \lambda_D)$: Here, the gyroradius is smaller than the Debye length but larger than the Landau length. In this regime, the magnetic field strongly influences collisions between the particles

8

This is the author's peer reviewed, accepted manuscript. However, the online version of record will be different from this version once it has been copyedited and typeset

PLEASE CITE THIS ARTICLE AS DOI: 10.1063/5.0146417

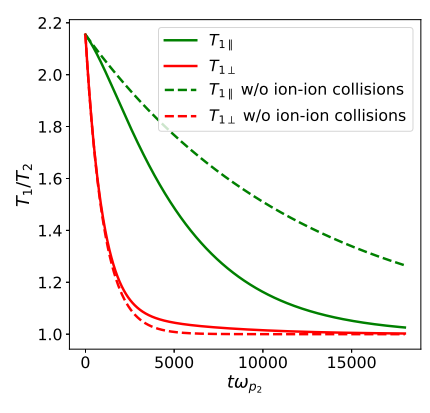


FIG. 7: The parallel and perpendicular ion temperature evolution when warm ions collisionally relax with a heat bath of electrons. Here, the electron coupling strength is $\Gamma_2=1$ and magnetization strength is $\beta_2=10$. Solid lines are for the case where both the ion-electron and ion-ion collisions are present and dashed lines are for the case where ion-ion collisions are turned off.

in addition to the macroscopic evolution of the distribution function. 4) The extremely magnetized regime $(r_c < \min\{r_L, \lambda_{\rm col}, a\})$: In this regime, the magnetic field is so strong that the gyroradius is the smallest length scale. Here, the motion of the particles is nearly 1D, with particles making 180° collisions at the distance of closest approach. Note that at strong coupling $(\Gamma > 1)$, the Coulomb collision mean free path becomes smaller than the Debye length and Landau length leading to the collapse of the four transport regimes to only two - the unmagnetized and extremely magnetized.²

As expected, the parallel and perpendicular temperature relaxation rates are independent of the magnetic field strength and have the same value through the unmagnetized and weakly magnetized regimes (1 and 2). The independence of the relaxation rates on the magnetic field is expected because the generalized collision operator in these regimes is equivalent to the traditional Boltzmann collision operator, which does not depend on the magnetic field strength. ¹⁶ In contrast, the parallel and perpendicular relaxation rates depend on the magnetic field strength and take different values from one another in the strongly and extremely magnetized regimes. The difference in the relaxation rates can cause anisotropy to form in the ion temperature during the collisional relaxation to thermal equilibrium. For like-charged interactions, strong magnetization increases both the parallel and perpendicular temperature relaxation rates (though by differing amounts), reaching constant values in the large β limit. A strikingly different behaviour is observed in the case of oppositely charged interactions, where although the perpendicular relaxation rate increases, the parallel relaxation rate decreases at a rate inversely proportional to β : $\nu_{\parallel} \propto \beta^{-1}$. This leads to a dramatic suppression of energy exchange along the magnetic field at high values of the magnetization strength.

V. DISCUSSION

This section discusses the temperature evolution of warm ions cooling down on a cool bath of electrons. The density of the background electrons (lighter species) is taken as much larger than the ion density so it can be considered a heat bath (i.e., constant temperature). This case is representative of anti-matter traps where antiprotons are mixed with electrons at the cooling stage (repulsive case) and with positrons during antihydrogen formation (attractive case) $^{25-27}$.

When there is an anisotropy in the ion temperature, ion-ion collisions reduce the anisotropy. Thus, when considering the ion temperature evolution, in addition to the ion-electron collisions, contributions from ion-ion collisions are included as a collision term in the Boltzmann equation. The temperature evolution equation of the ions then takes the following form.

$$\frac{dT_{1\perp}}{dt} = -\nu_{\perp} (T_{1\perp} - T_2) - \nu_A (T_{1\perp} - T_{1\parallel})$$

$$\frac{dT_{1\parallel}}{dt} = -\nu_{\parallel} (T_{1\parallel} - T_2) + 2\nu_A (T_{1\perp} - T_{1\parallel})$$
(20)

where ν_A is the anisotropy relaxation rate due to ionion interactions. Since ions are weakly magnetized, we use the relaxation rates from Ref. 46, obtained using the traditional Boltzmann collision operator to model this

$$\begin{split} \frac{\nu_A}{\bar{\nu}} &= \frac{3\sqrt{\pi}}{16} \frac{(1 + \frac{2}{3}A)^{3/2}}{\sqrt{\alpha}A^{5/2}} \int_0^\infty d\xi \xi^2 e^{-\alpha \xi^2} \frac{\sigma^{(2)}}{\sigma_0} \\ &\times \left[\frac{2}{3} \xi^2 \alpha A \text{erf}(\xi \sqrt{\alpha A}) - \psi(\xi^2 \alpha A) \right]. \end{split} \tag{22}$$

Here, $\sigma_0 \equiv \pi e^4/(2k_BT)^2$, $\xi^2 \equiv u^2/(2v_{T1}^2)$, $A \equiv T_{1\perp}/T_{1\parallel} - 1$, $\alpha \equiv \frac{1}{3}(3 + 2A)/(1 + A)$, $\bar{\nu} = 2\sqrt{\pi/m_1}n_1e^4/(k_BT_1)^{3/2}$ is the reference collision frequency, $\sigma^{(2)}$ is the $2^{\rm nd}$ momentum scattering cross section obtained using the potential of mean force computed from the HNC approximation for the one component plasma [Eq. (27) in Ref. 46] and

$$\psi(x) = \operatorname{erf}(\sqrt{x}) - \frac{2}{\sqrt{\pi}} \sqrt{x} e^{-x}$$
 (23)

is the Maxwell integral.

The temperature evolution obtained by integrating Eqs. (20) and (21)] is shown in Fig. 7. The plots are for the attractive (+-) interaction. As the previous section shows, electron-ion collisions lead to different temperature relaxation rates in the perpendicular and parallel

9

This is the author's peer reviewed, accepted manuscript. However, the online version of record will be different from this version once it has been copyedited and typeset PLEASE CITE THIS ARTICLE AS DOI: 10.1063/5.0146417

directions. Thus, as a warm ion distribution collisionally relaxes with electrons toward the equilibrium temperature, a temperature anisotropy develops. The dashed lines are the results of solving the equations without the ion-ion collisions, and solid lines account for both the ion-electron and ion-ion collisions. Here, the initial ion distribution is an isotropic Maxwellian distribution with a temperature, $T_1/T_2 = 2.1$, and the electrons are assumed to have a coupling strength, $\Gamma_2 = 1$, and magnetization strength, $\beta_2 = 10$. The density ratio of ions to electrons is $n_1/n_2 = 10^{-2}$. Even though the initial distribution is isotropic, the ion-electron collisional relaxation rate differs in the perpendicular and parallel directions. inducing temperature anisotropy during the relaxation process. Since the perpendicular energy equilibration rate is much larger than the parallel, the anisotropy is such that the parallel temperature is larger through the evolution. This anisotropy is slightly relaxed by ion-ion collisions. Here, the temperature evolution is obtained by assuming that the ion distribution stays an anisotropic Maxwellian throughout the evolution. This assumption simplifies the energy moment of the Boltzmann equation to Eqs. (12) and (13). A more general solution of the full kinetic equation may predict deviations from this assumed form, but it is expected to provide an accurate approximation for sufficiently small differences between the electron and ion temperatures.

VI. CONCLUSION

This work used the recently developed generalized Boltzmann kinetic theory for strongly magnetized plasmas to calculate the ion-electron temperature relaxation rate. The temperature relaxation rate was obtained from the energy exchange density of a test charge slowing down in a strongly magnetized plasma. It was found that when the plasma is strongly magnetized, the relaxation rates change and also cause the rates in the parallel and perpendicular directions to no longer be equal. Different parallel and perpendicular temperature relaxation rates cause temperature anisotropy to develop when the ions and electrons equilibrate to a common temperature. The relaxation rates were also found to depend on the sign of the charge of the interacting particles, known as the Barkas effect. The Barkas effect increases the difference between the parallel and perpendicular relaxation rates. The parallel relaxation rate in the case of oppositely charged interaction was found to be inversely proportional to the magnetic field strength in the strongly magnetized regime.

These new results may be observed in magnetized plasma experiments, including ultra-cold neutral plasmas^{5,8,9} and antimatter traps³. Modeling these experiments requires the computation of macroscopic transport coefficients like diffusion^{1,2,47,48}, conductivity⁴⁹, shear viscosity⁵⁰, and other characteristics like dynamic structure factor 51 . The generalized collision operator is a strong candidate for obtaining them. This will be explored in future work.

VII. DATA AVAILABILITY STATEMENT

The data that support the findings of this study are available from the corresponding author upon reasonable request.

VIII. AUTHOR DECLARATIONS

A. Conflict of Interest

The authors have no conflicts to disclose.

ACKNOWLEDGMENTS

The authors thank Dr. David J. Bernstein for helpful conversations during the development of this work. This material is based upon work supported by the U.S. DOE under grant award No. DE-SC0022202 and NSF grant award No. PHY-2205506. It used Expanse at San Diego Supercomputer Center through allocation PHY-150018 from the Advanced Cyberinfrastructure Coordination Ecosystem: Services & Support (ACCESS) program, which is supported by National Science Foundation grants #2138259, #2138286, #2138307, #2137603, and #2138296

- ¹T. Ott and M. Bonitz, "Diffusion in a strongly coupled magnetized plasma," Physical review letters 107, 135003 (2011).
- ²S. D. Baalrud and J. Daligault, "Transport regimes spanning magnetization-coupling phase space," Phys. Rev. E 96, 043202
- July 17. July 17. Specifical S ⁴E. V. Stenson, J. Horn-Stanja, M. R. Stoneking, and T. S. Pedersen, "Debve length and plasma skin depth: two length scales of interest in the creation and diagnosis of laboratory pair plasmas,
- Journal of Plasma Physics 83, 595830106 (2017).

 ⁵G. M. Gorman, M. K. Warrens, S. J. Bradshaw, and T. C. Killian, "Laser-induced-fluorescence imaging of a spin-polarized ultracold neutral plasma in a magnetic field," Phys. Rev. A 105, 013108 (2022).
- ⁶G. M. Gorman, M. K. Warrens, S. J. Bradshaw, and T. C. Killian, "Magnetic confinement of an ultracold neutral plasma," Phys Rev. Lett. 126, 085002 (2021)
- X. L. Zhang, R. S. Fletcher, S. L. Rolston, P. N. Guzdar, and M. Swisdak, "Ultracold plasma expansion in a magnetic field," Phys. Rev. Lett. 100, 235002 (2008)
- ⁸R. T. Sprenkle, S. D. Bergeson, L. G. Silvestri, and M. S. Murillo, "Ultracold neutral plasma expansion in a strong uniform magnetic field," Phys. Rev. E **105**, 045201 (2022).

 ⁹J. M. Guthrie and J. L. Roberts, "Finite-amplitude rf heating
- rates for magnetized electrons in neutral plasma," Physics of Plasmas 28, 052101 (2021), https://doi.org/10.1063/5.0047640.
- ¹⁰B. R. Beck, J. Fajans, and J. H. Malmberg, "Measurement of collisional anisotropic temperature relaxation in a strongly magnetized pure electron plasma," Phys. Rev. Lett. $\mathbf{68}, 317 – 320 \ (1992)$

accepted manuscript. However, the online version of record will be different from this version once it has been copyedited and typeset This is the author's peer reviewed,

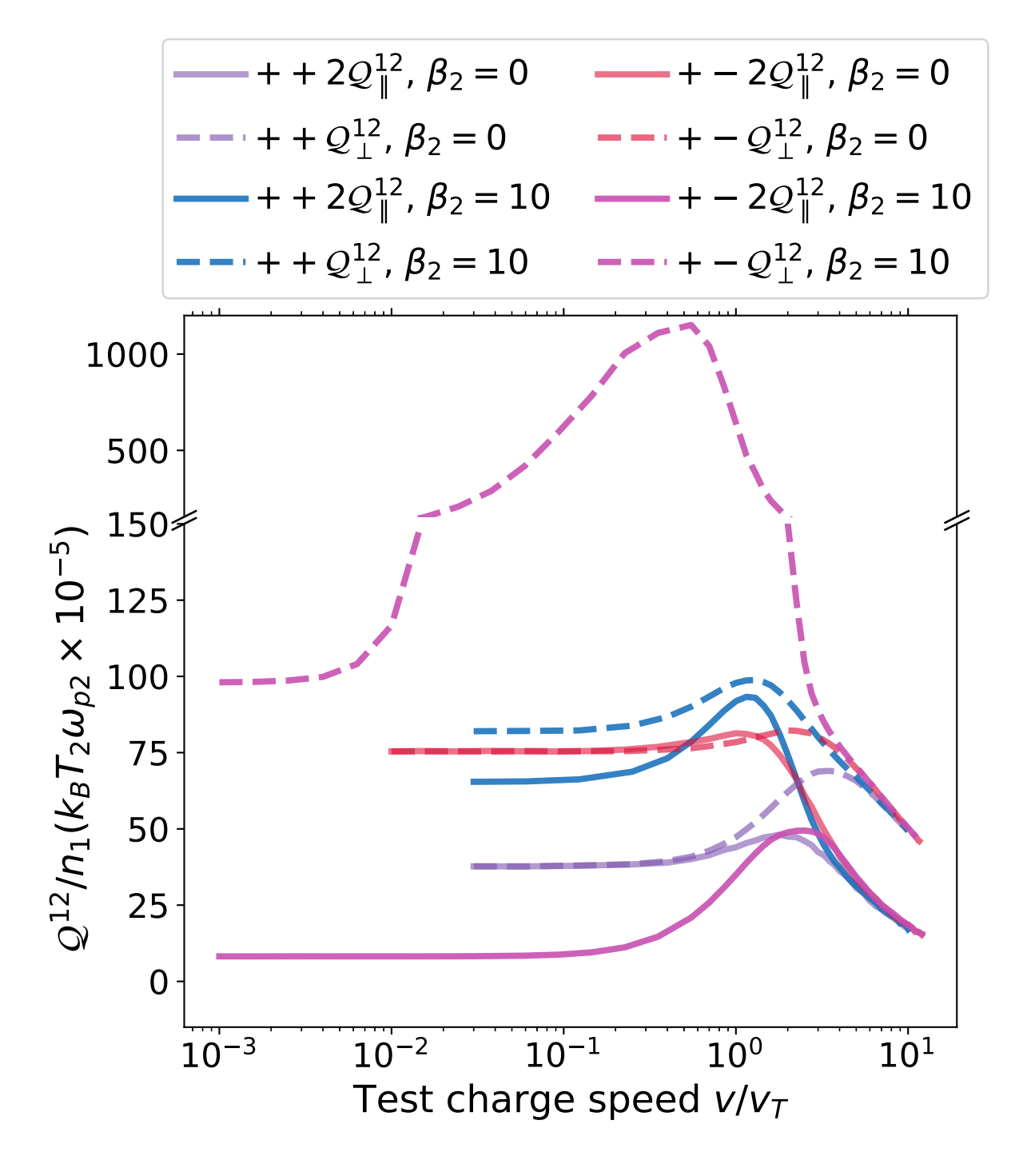
PLEASE CITE THIS ARTICLE AS DOI: 10.1063/5.0146417

- ¹¹E. Thomas, R. L. Merlino, and M. Rosenberg, "Magnetized dusty plasmas: the next frontier for complex plasma research," Plasma Physics and Controlled Fusion 54, 124034 (2012).
- ¹² N. Bennett, D. R. Welch, G. Laity, D. V. Rose, and M. E. Cuneo, "Magnetized particle transport in multi-ma accelerators," Phys. Rev. Accel. Beams 24, 060401 (2021).
- A. Aymar, P. Barabaschi, and Y. Shimomura, "The ITER design," Plasma Physics and Controlled Fusion 44, 519–565 (2002).
 J. H. Ferziger and H. G. Kaper, Mathematical theory of transport
- processes in gases (North-Holland, 1972).

 15S. Ichimaru, Statistical Plasma Physics, Volume I: Basic Principles (CRC Press, 2004).
- ¹⁶L. Jose and S. D. Baalrud, "A generalized boltzmann kinetic theory for strongly magnetized plasmas with application to friction," Physics of Plasmas 27, 112101 (2020).
- ¹ Tu. Jose and S. D. Baalrud, "A kinetic model of friction in strongly coupled strongly magnetized plasmas," Physics of Plasmas 28, 072107 (2021), https://doi.org/10.1063/5.0054552.
- ¹⁸Y. S. Derbenev and A. N. Skrinsky, "The Effect of an Accompanying Magnetic Field on Electron Cooling," Part. Accel. 8, 235–243 (1978).
- I. Menshikov, "New directions in the theory of electron cooling," Physics-Uspekhi 51, 645–680 (2008).
 V. Parkhomchuk, "Study of fast electron cooling," in *Proceedings*
- ²⁰V. Parkhomchuk, "Study of fast electron cooling," in *Proceedings of the Workshop on Electron Cooling and Related Applications (ECOOL84, 1984)*, edited by H. Poth (Kernforschungszentrum Karlsruhe GmbH, Karlsruhe, 1984) pp. 71–84.
- ²¹T. Lafleur and S. D. Baalrud, "Transverse force induced by a magnetized wake," Plasma Physics and Controlled Fusion 61, 125004 (2019).
- ²²T. Lafleur and S. D. Baalrud, "Friction in a strongly magnetized neutral plasma," Plasma Physics and Controlled Fusion 62, 095003 (2020).
- ²³D. J. Bernstein, T. Lafleur, J. Daligault, and S. D. Baalrud, "Friction force in strongly magnetized plasmas," Phys. Rev. E 102, 041201 (2020).
- 102, 041201 (2020).
 L. Jose, D. J. Bernstein, and S. D. Baalrud, "Barkas effect in strongly magnetized plasmas," Physics of Plasmas 29, 112103 (2022), https://doi.org/10.1063/5.0121285.
 M. Ahmadi, B. X. R. Alves, C. J. Baker, W. Bertsche, E. But-
- ²⁹M. Ahmadi, B. X. R. Alves, C. J. Baker, W. Bertsche, E. Butler, A. Capra, C. Carruth, C. L. Cesar, M. Charlton, S. Cohen, R. Collister, S. Eriksson, A. Evans, N. Evetts, J. Fajans, T. Friesen, M. C. Fujiwara, D. R. Gill, A. Gutierrez, J. S. Hangst, W. N. Hardy, M. E. Hayden, C. A. Isaac, A. Ishida, M. A. Johnson, S. A. Jones, S. Jonsell, L. Kurchaninov, N. Madsen, M. Mathers, D. Maxwell, J. T. K. McKenna, S. Menary, J. M. Michan, T. Momose, J. J. Munich, P. Nolan, K. Olchanski, A. Olin, P. Pusa, C. Ø. Rasmussen, F. Robicheaux, R. L. Sacramento, M. Sameed, E. Sarid, D. M. Silveira, S. Stracka, G. Stutter, C. So, T. D. Tharp, J. E. Thompson, R. I. Thompson, D. P. van der Werf, and J. S. Wurtele, "Antihydrogen accumulation for fundamental symmetry tests," Nature Communications 8, 681 (2017).
- 26 C. J. Baker, W. Bertsche, A. Capra, C. L. Cesar, M. Charlton, A. C. Mathad, S. Eriksson, A. Evans, N. Evetts, S. Fabbri, J. Fajans, T. Friesen, M. C. Fujiwara, P. Grandemange, P. Granum, J. S. Hangst, M. E. Hayden, D. Hodgkinson, C. A. Isaac, M. A. Johnson, J. M. Jones, S. A. Jones, S. Jonsell, L. Kurchaninov, N. Madsen, D. Maxwell, J. T. K. McKenna, S. Menary, T. Momose, P. Mullan, K. Olchanski, A. Olin, J. Peszka, A. Powell, P. Pusa, C. Ø. Rasmussen, F. Robicheaux, R. L. Sacramento, M. Sameed, E. Sarid, D. M. Silveira, G. Stutter, C. So, T. D. Tharp, R. I. Thompson, D. P. van der Werf, and J. S. Wurtele, "Sympathetic cooling of positrons to cryogenic temperatures for antihydrogen production," Nature Communications 12, 6139 (2021).
- ²⁷W. A. Bertsche, E. Butler, M. Charlton, and N. Madsen, "Physics with antihydrogen," Journal of Physics B: Atomic, Molecular and Optical Physics 48, 232001 (2015).
- $^{28}\mathrm{S.}$ Ichimaru and M. N. Rosenbluth, "Relaxation processes in plasmas with magnetic field. temperature re-

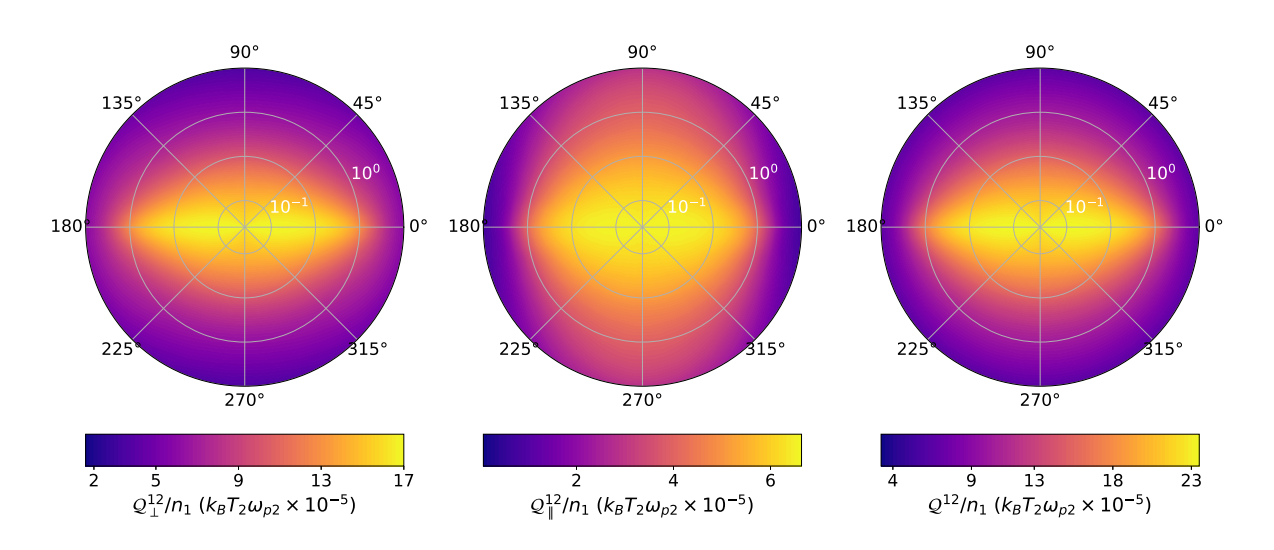
- laxations," The Physics of Fluids **13**, 2778–2789 (1970), https://aip.scitation.org/doi/pdf/10.1063/1.1692864.
- ²⁹H. B. Nersisyan, C. Deutsch, and A. K. Das, "Number-conserving linear-response study of low-velocity ion stopping in a collisional magnetized classical plasma," Phys. Rev. E 83, 036403 (2011).
- ³⁰T. Kihara, Y. Midzuno, K. Sakuma, and T. Shizume, "Ion-electron relaxation of plasmas in a magnetic field, ii." Journal of the Physical Society of Japan 15, 684–687 (1960), https://doi.org/10.1143/JPSJ.15.684.
- ³¹T. Kihara and Y. Midzuno, "Irreversible processes in plasmas in a strong magnetic field," Rev. Mod. Phys. **32**, 722–730 (1960).
- ³²C. Dong, H. Ren, H. Cai, and D. Li, "Effects of magnetic field on anisotropic temperature relaxation," Physics of Plasmas 20, 032512 (2013).
- ³³C. Dong, H. Ren, H. Cai, and D. Li, "Temperature relaxation in a magnetized plasma," Physics of Plasmas 20, 102518 (2013).
- ³⁴T. Kihara, "Ion-electron relaxation of plasmas in a strong magnetic field. i," Journal of the Physical Society of Japan 14, 1751-1754 (1959), https://doi.org/10.1143/JPSJ.14.1751.
- ³⁵V. Silin, "On relaxation of electron and ion temperatures of fully ionized plasma in a strong magnetic field," Sov. Phys. JETP 16, 1281 (1963).
- ³⁶S. D. Baalrud and J. Daligault, "Mean force kinetic theory: A convergent kinetic theory for weakly and strongly coupled plasmas," Physics of Plasmas 26, 082106 (2019).
- ³⁷S. D. Baalrud and J. Daligault, "Effective potential theory for transport coefficients across coupling regimes," Phys. Rev. Lett. 110, 235001 (2013).
- ³⁸D. J. Bernstein, S. D. Baalrud, and J. Daligault, "Effects of coulomb coupling on stopping power and a link to macroscopic transport," Physics of Plasmas 26, 082705 (2019).
- ³⁹D. J. Bernstein and S. D. Baalrud, "Method to determine the electron—ion temperature relaxation rate from test particle distributions," Physics of Plasmas 29, 072705 (2022).
- ⁴⁰S. D. Baalrud and J. Daligault, "Extending plasma transport theory to strong coupling through the concept of an effective interaction potential," Physics of Plasmas 21, 055707 (2014).
- ⁴¹J. P. Hansen and I. R. McDonald, Theory of simple liquids: with applications to soft matter (Academic Press, 2013).
- applications to soft matter (Academic Press, 2013). $^{42}\mathrm{G.~P.~Lepage}$, "Adaptive multidimensional integration: vegas enhanced," Journal of Computational Physics $\mathbf{439},\,110386$ (2021).
- Lepage, "gplepage/vegas: vegas version 3.4.2," (2020).
 E. Hairer, S. P. Norsett, and G. Wanner, "Runge-kutta and extrapolation methods," in Solving Ordinary Differential Equations I: Nonstiff Problems (Springer Berlin Heidelberg, 1993) pp. 129–353.
- ⁴⁵N. R. Shaffer and S. D. Baalrud, "The barkas effect in plasma transport," Physics of Plasmas 26, 032110 (2019), https://doi.org/10.1063/1.5089140.
- ⁴⁶S. D. Baalrud and J. Daligault, "Temperature anisotropy relaxation of the one-component plasma," Contributions to Plasma Physics 57, 238–251 (2017), https://onlinelibrary.wiley.com/doi/pdf/10.1002/ctpp.201700028.
- ⁴⁷D. H. Dubin, "Parallel velocity diffusion and slowing-down rate from long-range collisions in a magnetized plasma," Physics of Plasmas 21, 052108 (2014).
- ⁴⁸D. H. E. Dubin, "Test particle diffusion and the failure of integration along unperturbed orbits," Phys. Rev. Lett. **79**, 2678–2681 (1997).
- T. Ott, M. Bonitz, P. Hartmann, and Z. Donkó, "Spontaneous generation of temperature anisotropy in a strongly coupled magnetized plasma," Phys. Rev. E 95, 013209 (2017).
 B. Scheiner and S. D. Baalrud, "Viscosity of the magnetized
- ⁵⁰B. Scheiner and S. D. Baalrud, "Viscosity of the magnetized strongly coupled one-component plasma," Phys. Rev. E 102, 063202 (2020).
- ⁵¹H. Kählert and M. Bonitz, "Dynamic structure factor of the magnetized one-component plasma: Crossover from weak to strong coupling," Phys. Rev. Res. 4, 013197 (2022).

PLEASE CITE THIS ARTICLE AS DOI: 10.1063/5.0146417



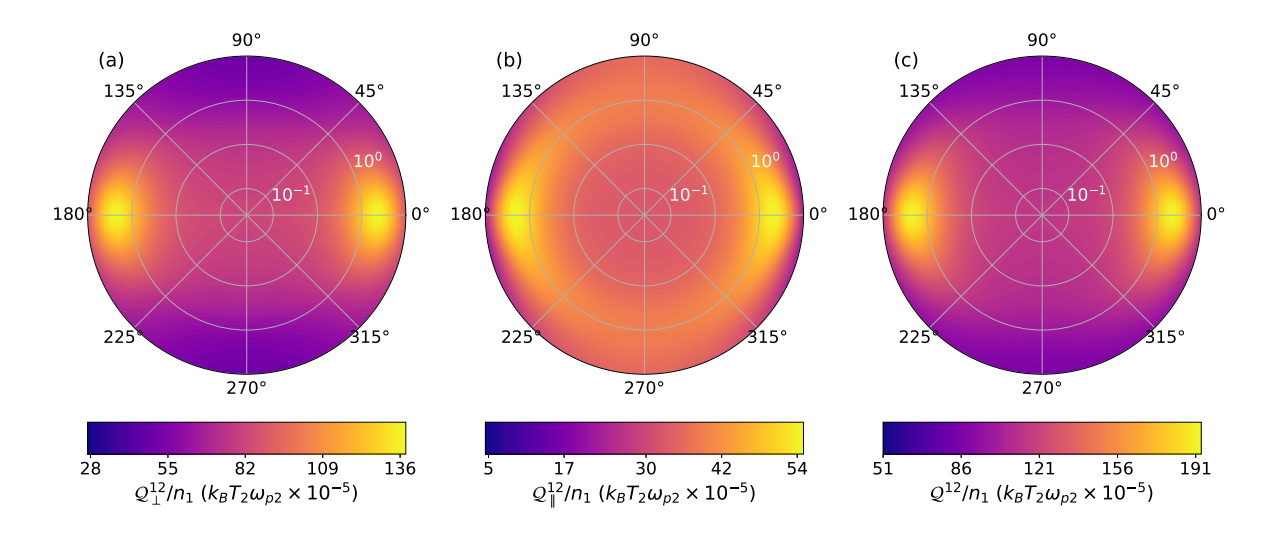
This is the author's peer reviewed, accepted manuscript. However, the online version of record will be different from this version once it has been copyedited and typeset.

PLEASE CITE THIS ARTICLE AS DOI: 10.1063/5.0146417



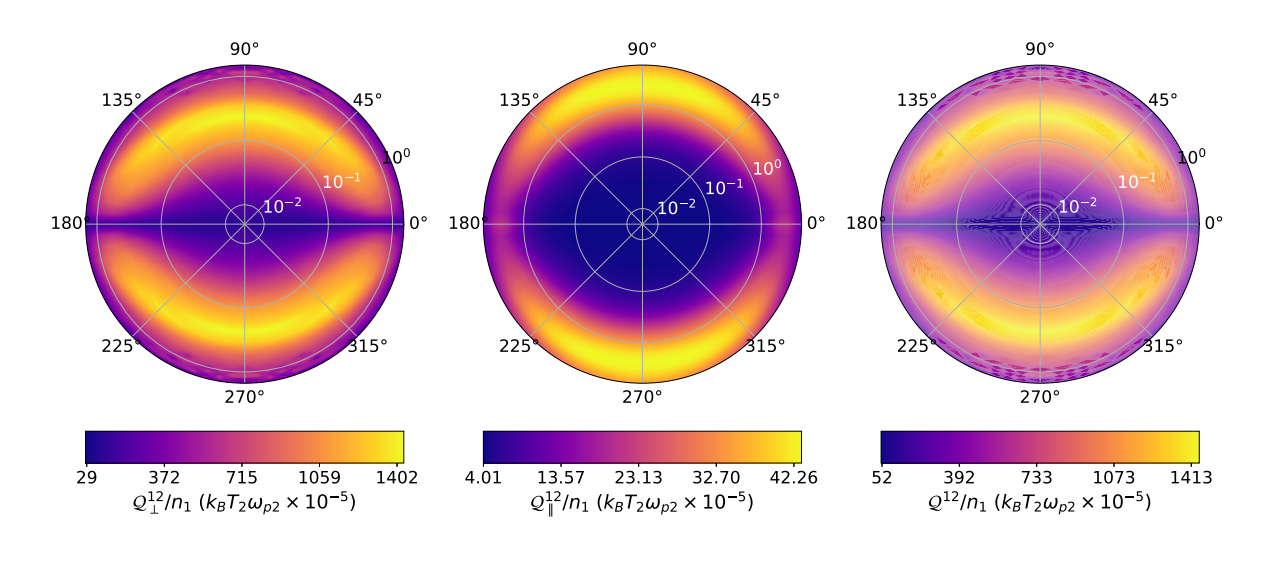
This is the author's peer reviewed, accepted manuscript. However, the online version of record will be different from this version once it has been copyedited and typeset.

PLEASE CITE THIS ARTICLE AS DOI: 10.1063/5.0146417



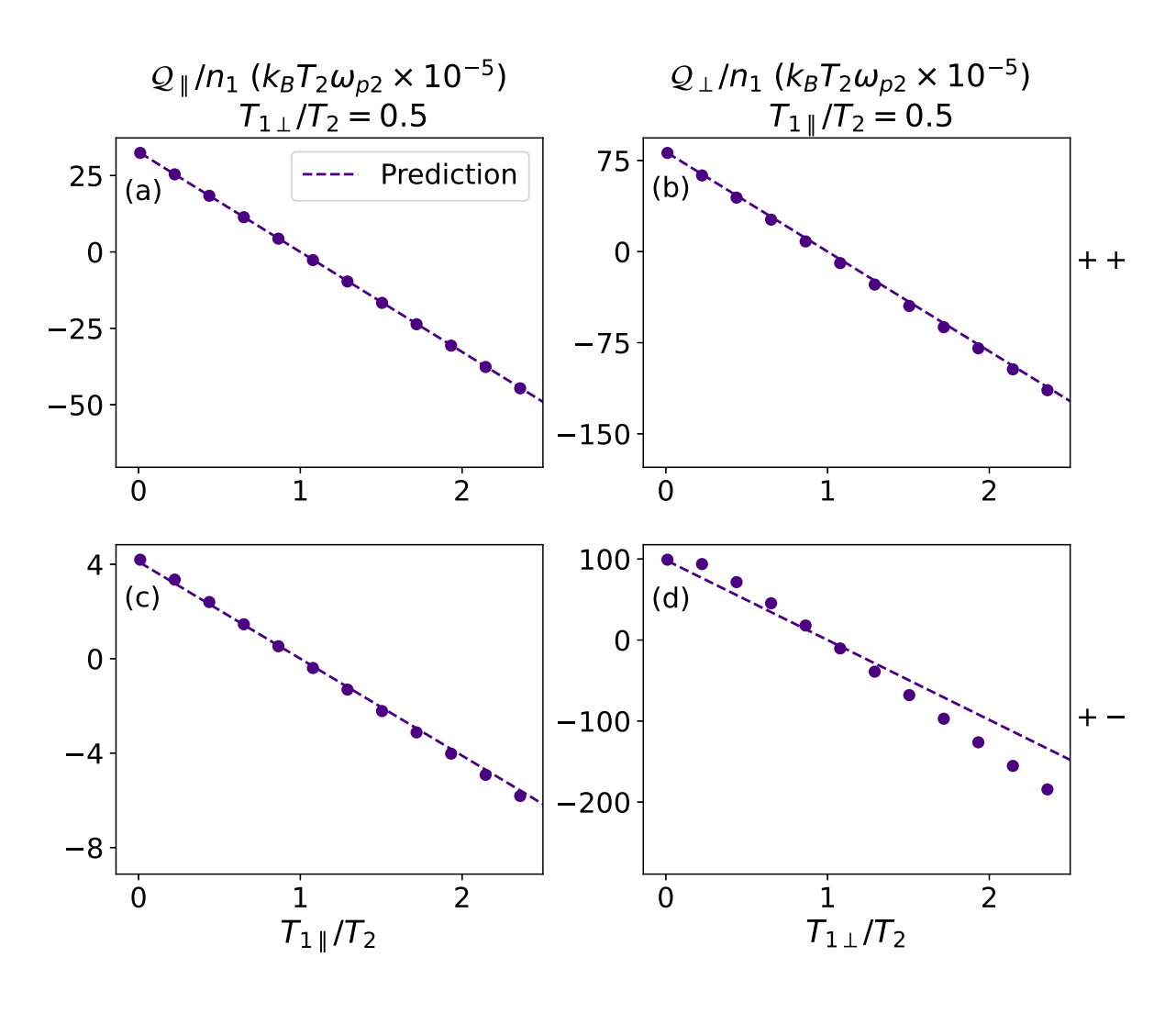
This is the author's peer reviewed, accepted manuscript. However, the online version of record will be different from this version once it has been copyedited and typeset.

PLEASE CITE THIS ARTICLE AS DOI: 10.1063/5.0146417

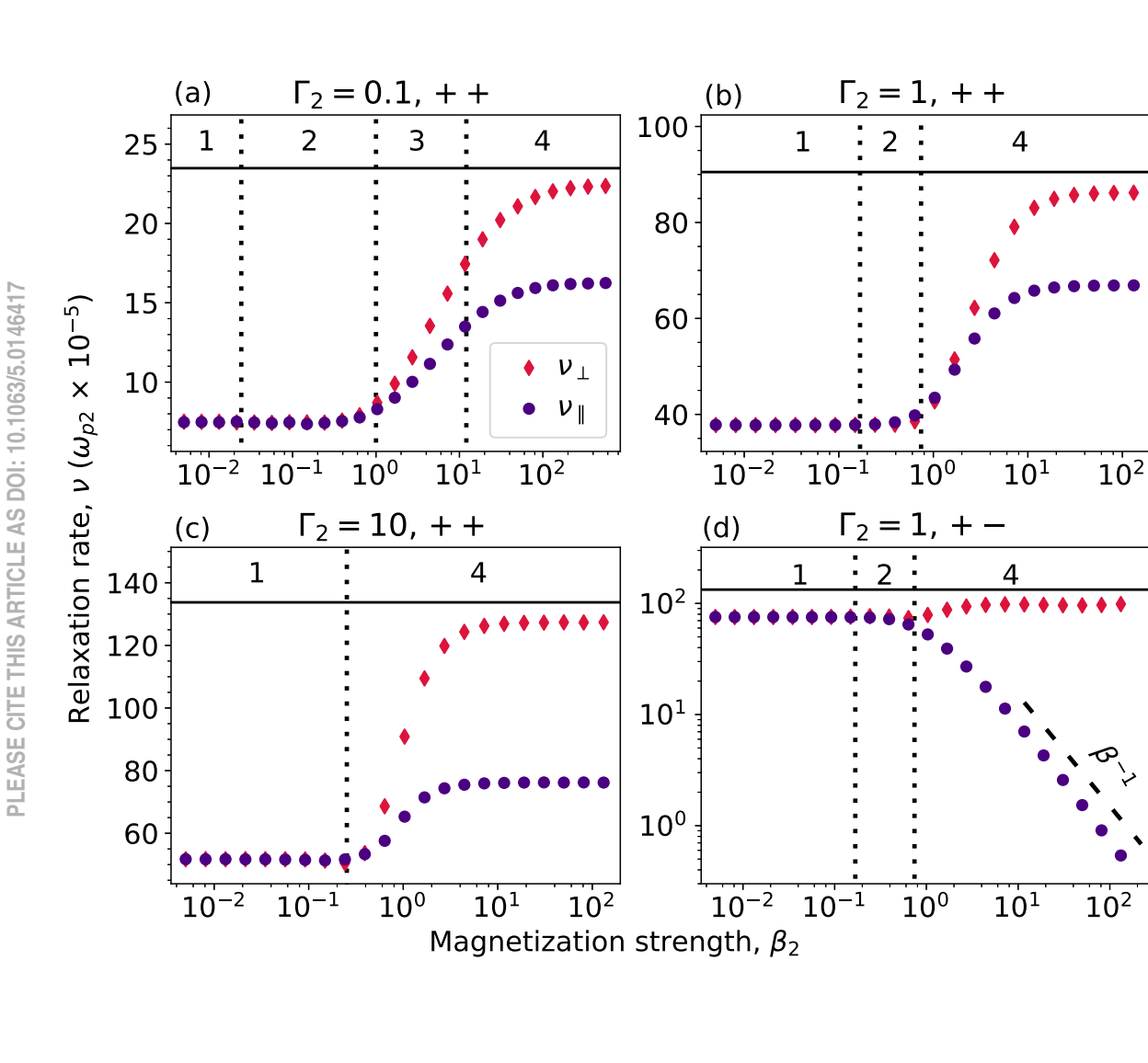


This is the author's peer reviewed, accepted manuscript. However, the online version of record will be different from this version once it has been copyedited and typeset.





This is the author's peer reviewed, accepted manuscript. However, the online version of record will be different from this version once it has been copyedited and typeset.



This is the author's peer reviewed, accepted manuscript. However, the online version of record will be different from this version once it has been copyedited and typeset.



